

This is a self-archived version of an original article. This version may differ from the original in pagination and typographic details.

Author(s): ALICE Collaboration

Title: Characterizing the initial conditions of heavy-ion collisions at the LHC with mean transverse momentum and anisotropic flow correlations

Year: 2022

Version: Published version

Copyright: © 2022 The Author(s). Published by Elsevier B.V.

Rights: CC BY 4.0

Rights url: <https://creativecommons.org/licenses/by/4.0/>

Please cite the original version:

ALICE Collaboration. (2022). Characterizing the initial conditions of heavy-ion collisions at the LHC with mean transverse momentum and anisotropic flow correlations. *Physics Letters B*, 834, Article 137393. <https://doi.org/10.1016/j.physletb.2022.137393>



Characterizing the initial conditions of heavy-ion collisions at the LHC with mean transverse momentum and anisotropic flow correlations



ALICE Collaboration*

ARTICLE INFO

Article history:

Received 17 May 2022

Received in revised form 23 July 2022

Accepted 20 August 2022

Available online 24 August 2022

Editor: M. Doser

ABSTRACT

Correlations between mean transverse momentum $\langle p_T \rangle$ and anisotropic flow coefficients v_2 or v_3 are measured as a function of centrality in Pb–Pb and Xe–Xe collisions at $\sqrt{s_{NN}} = 5.02$ TeV and 5.44 TeV, respectively, with ALICE. In addition, the recently proposed higher-order correlation between $\langle p_T \rangle$, v_2 , and v_3 is measured for the first time, which shows an anticorrelation for the presented centrality ranges. These measurements are compared with hydrodynamic calculations using IP-Glasma and T_RENTo initial-state shapes, the former based on the Color Glass Condensate effective theory with gluon saturation, and the latter a parameterized model with nucleons as the relevant degrees of freedom. The data are better described by the IP-Glasma rather than the T_RENTo based calculations. In particular, Trajectum and JETSCAPE predictions, both based on the T_RENTo initial state model but with different parameter settings, fail to describe the measurements. As the correlations between $\langle p_T \rangle$ and v_n are mainly driven by the correlations of the size and the shape of the system in the initial state, these new studies pave a novel way to characterize the initial state and help pin down the uncertainty of the extracted properties of the quark–gluon plasma recreated in relativistic heavy-ion collisions.

© 2022 The Author(s). Published by Elsevier B.V. This is an open access article under the CC BY license (<http://creativecommons.org/licenses/by/4.0/>). Funded by SCOAP³.

The primary goal of ultrarelativistic heavy-ion collisions is to study the quark–gluon plasma (QGP) [1], a deconfined state of quarks and gluons, predicted by quantum chromodynamics (QCD) to emerge at extreme densities and temperatures. High-energy heavy-ion collisions at Relativistic Heavy Ion Collider (RHIC) [2–5] and the Large Hadron Collider (LHC) at CERN [6,7] have yielded strong evidence that the QGP is observed in such collisions, enabling the study of its properties in the laboratory. A key phenomenon that provides valuable information on the transport properties of the created QGP matter is the anisotropic expansion of the produced particles [8]. The final anisotropy can be quantified by a Fourier decomposition of the single particle azimuthal distribution [9],

$$P(\varphi) = \frac{1}{2\pi} \left[1 + 2 \sum_{n=1}^{\infty} v_n \cos n(\varphi - \Psi_n) \right]. \quad (1)$$

Here, φ is the azimuthal angle of the emitted particle, and v_n and Ψ_n are the n -th order flow coefficient and flow symmetry-plane angle, respectively. Systematic measurements on fluctuations and correlations of v_n coefficients and Ψ_n have been previously reported in Refs. [10–25]. Comprehensive comparisons with hydrodynamic model calculations provide critical information on the

event average initial-state shape and the initial energy density distribution in the nuclear overlap region, as well as their event-by-event fluctuations. Additionally, they constrain the shear and bulk viscosity over entropy density ratios of the QGP, η/s and ζ/s , respectively [26–29]. Even at fixed final-state particle multiplicity, not only the shape but also the average size of the nuclear overlap region will, in general, fluctuate from event to event. These size fluctuations (at constant charged-particle density) lead to fluctuations of the pressure gradient and therefore affect the radial flow, thus influencing the transverse momentum (p_T) spectra of the produced particles. Arguably, the event-by-event fluctuations of the mean transverse momentum $\langle p_T \rangle$ (the average transverse momentum of all particles in a single event) are more sensitive to the equation-of-state and ζ/s than the measurements of the anisotropic flow [30,31]. Despite their early success in describing v_n measurements, hydrodynamic models have been able to reproduce the observed $\langle p_T \rangle$ fluctuations only recently [32–34]. Notably the measurements of v_n and $\langle p_T \rangle$ are used as independent experimental inputs for the Bayesian analyses [33–36], which extract state-of-the-art information on the initial conditions and the final state properties, including the temperature dependence of η/s and ζ/s .

Apart from the individual studies of v_n and $\langle p_T \rangle$, the interplay between radial and anisotropic flow was qualitatively investigated via anisotropic flow of identified hadrons [37,38] and with event-shape engineering (ESE) [39]. It was proposed that correlations

* E-mail address: alice-publications@cern.ch.

between radial and anisotropic flow could be quantified via correlations between $[p_T]$ and v_n using a modified Pearson correlation coefficient [40],

$$\rho(v_n^2, [p_T]) = \frac{\text{Cov}(v_n^2, [p_T])}{\sqrt{\text{Var}(v_n^2)} \sqrt{c_k}}, \quad (2)$$

where $\text{Cov}(v_n^2, [p_T])$ is the covariance between v_n^2 and $[p_T]$, it can be calculated using a three-particle correlation following Eq. (1) in Ref. [40]. The variance of v_n^2 fluctuations is given by $\text{Var}(v_n^2)$ and can be measured by two- and four-particle cumulants, $\text{Var}(v_n^2) = v_n\langle 2 \rangle^4 - v_n\langle 4 \rangle^4$. Dynamical transverse momentum correlations are given by c_k [40–43]. As $\rho(v_n^2, [p_T])$ (for $n = 2, 3$) can be qualitatively or even quantitatively reproduced by the initial state correlations [31,44,45], its measurements will provide valuable information on the overlap region's shape and size, and their correlations in the initial conditions. In particular, $\rho(v_2^2, [p_T])$ is found to be sensitive to the nuclear quadrupole deformation [46], adding a new tool to study the nuclear structure, which has been addressed systematically only at low energies so far [47]. This $\rho(v_n^2, [p_T])$ (for $n = 2, 3, 4$) observable has been measured previously [48], which reported a clear dependence on charged-particle multiplicity, when selecting particles with $p_T > 0.5$ GeV/c.

Recently, a new observable that probes the correlations between $[p_T]$ and two different v_m^2 and v_n^2 coefficients has been introduced [49]. This observable $\rho(v_m^2, v_n^2, [p_T])$ can be achieved by replacing three observables A, B, and C with v_m^2 , v_n^2 , and $[p_T]$ in Eq. (24) from Ref. [49],

$$\rho(v_m^2, v_n^2, [p_T]) = \frac{\text{Cor}(v_m^2, v_n^2, [p_T])}{\sqrt{\text{Var}(v_m^2)} \sqrt{\text{Var}(v_n^2)} \sqrt{c_k}} - \frac{\langle v_m^2 \rangle}{\sqrt{\text{Var}(v_m^2)}} \cdot \rho_n - \frac{\langle v_n^2 \rangle}{\sqrt{\text{Var}(v_n^2)}} \cdot \rho_m - \frac{\langle [p_T] \rangle}{\sqrt{c_k}} \cdot \frac{SC(m, n)}{\sqrt{\text{Var}(v_m^2)} \sqrt{\text{Var}(v_n^2)}}, \quad (3)$$

where $\rho_i = \rho(v_i^2, [p_T])$, $\text{Cor}(v_m^2, v_n^2, [p_T])$ is the correlation among v_m^2 , v_n^2 , and $[p_T]$ defined in Ref. [49], and $SC(m, n)$ is the symmetric cumulant between v_m^2 and v_n^2 [16,50,51]. The $\rho(v_m^2, v_n^2, [p_T])$ is constructed based on multiparticle cumulants [49,52], where lower-order few particle correlations have been removed, thus, it only reflects the genuine correlations between $[p_T]$, v_n , and v_m . It is potentially more sensitive than $\rho(v_n^2, [p_T])$ to the initial conditions and is expected to be used to probe the initial momentum anisotropy [44], an asymmetry in the transverse pressure of the system at the interface between a pre-equilibrium description and a hydrodynamic description. The presence of an initial momentum anisotropy was predicted from first-principle considerations in the colour glass condensate (CGC) effective theory of high-energy QCD [53,54]. However, conclusive evidence for the CGC remains elusive.

In this Letter, the measurements of the centrality dependence of correlations between flow coefficients and $[p_T]$ in Pb–Pb and Xe–Xe collisions at 5.02 TeV and 5.44 TeV, respectively, are presented. The collision centrality is determined using energy deposition in the two scintillator arrays of the V0 detector, V0A and V0C, which cover the pseudorapidity ranges of $2.8 < \eta < 5.1$ and $-3.7 < \eta < -1.7$, respectively [55,56]. Events that pass central, semi-central, or minimum-bias trigger criteria with a reconstructed primary vertex (PV) within ± 10 cm of the nominal interaction point along the beam direction are used. Background events are removed using information from multiple detectors as described in Ref. [57]. A total of 245 million Pb–Pb collisions and 1.2 million Xe–Xe collisions pass these criteria. The charged-particle tracks are

reconstructed using the Inner Tracking System (ITS) [58] and the Time Projection Chamber (TPC) [59]. To select only high-quality reconstructed tracks for the analysis, they are required to be in the kinematic range $0.2 < p_T < 3.0$ GeV/c and $|\eta| < 0.8$, to have more than 70 TPC space points (out of a maximum of 159), and a χ^2 per degree of freedom of the track fit to the TPC space points to be lower than 2. In order to reduce the contamination from secondary particles, the distance-of-closest-approach (DCA) of the tracks to the PV must be within 2 cm in the longitudinal direction and a p_T -dependent distance selection in the transverse plane, ranging from 0.2 cm at $p_T = 0.2$ GeV/c to 0.02 cm at $p_T = 3.0$ GeV/c, is applied. To suppress the non-flow contaminations, which are the azimuthal angle correlations not associated to Ψ_n , multiparticle correlations with the subevent method [52,60] are applied. For this, the pseudorapidity acceptance of the central barrel is divided into three regions (subevents), A, B, and C, corresponding to $-0.8 < \eta_A < -0.4$, $|\eta_B| < 0.4$, and $0.4 < \eta_C < 0.8$, respectively. Here subevents A and C are used in the v_n measurements, while subevent B is used for $[p_T]$ measurements. The v_n , $[p_T]$, and their correlations are measured in each event and corrected for detector acceptance and track-reconstruction efficiency using the latest developments based on generic framework with 3-subevent method [50,60] including $[p_T]$ calculations.

Systematic uncertainties are estimated by varying event and track selection criteria. Uncertainties related to the selection of the event include the variation of the accepted vertex position along the beam line (9, 7 and 5 cm), and consideration of different magnetic field directions, which are analyzed separately. The resulting systematic uncertainty was found to be within 2%. The systematic uncertainties related to track selection criteria are estimated by considering different track reconstruction algorithms and reconstruction qualities. The variations of the maximum allowed DCA to the primary vertex along the beam line and in the transverse plane result in differences less than 1%. The quality of reconstructed tracks is varied by increasing the minimum number of space points in the TPC associated with the reconstructed track to 80 and 90, which leads to a negligible effect on the measured correlations. It is also found that the tracking efficiency exhibits a slight centrality dependence, varying by about 4% with multiplicity. To account for this, the tracking efficiency is varied by $\pm 4\%$ in a p_T -dependent way, so that the efficiency is at its nominal value at $p_T = 0.2$ GeV/c and 4% larger or smaller at $p_T = 3.0$ GeV/c. This yields a systematic uncertainty below 1%. The residual non-flow contaminations are studied with the 3-subevent method [60,61] and the effects are found to be negligible, which agrees with the findings from model studies [61]. Only the sources of systematic uncertainty found to be statistically significant by more than 1σ following the procedure introduced in Ref. [62] are added in quadrature to obtain the total systematic uncertainty.

The measurements of $\rho(v_2^2, [p_T])$ and $\rho(v_3^2, [p_T])$ as a function of collision centrality in Pb–Pb collisions at $\sqrt{s_{NN}} = 5.02$ TeV and Xe–Xe collisions at $\sqrt{s_{NN}} = 5.44$ TeV are presented in Fig. 1. In Pb–Pb and Xe–Xe collisions, $\rho(v_2^2, [p_T])$ has a weak centrality dependence and is positive in the considered centrality range. This implies that v_2 and $[p_T]$ are positively correlated and confirms the previous studies using the ESE approach [39]. The presented ALICE results also qualitatively agree with the previous ATLAS measurements [48]. The stronger centrality dependence reported by the ATLAS Collaboration might be attributed to the different kinematic selection criteria and the choice of centrality determination. Hydrodynamic model calculations from the v-USPhydro model [30], the Trajectory Bayesian analysis [35], the JETSCAPE Bayesian analysis [36], and the IP-Glasma+MUSIC+UrQMD model [31], whenever available, are compared to data. The width of the bands illustrated in Fig. 1 denotes the statistical uncertainty of the model calculations using maximum a posteriori (MAP) parametrization,

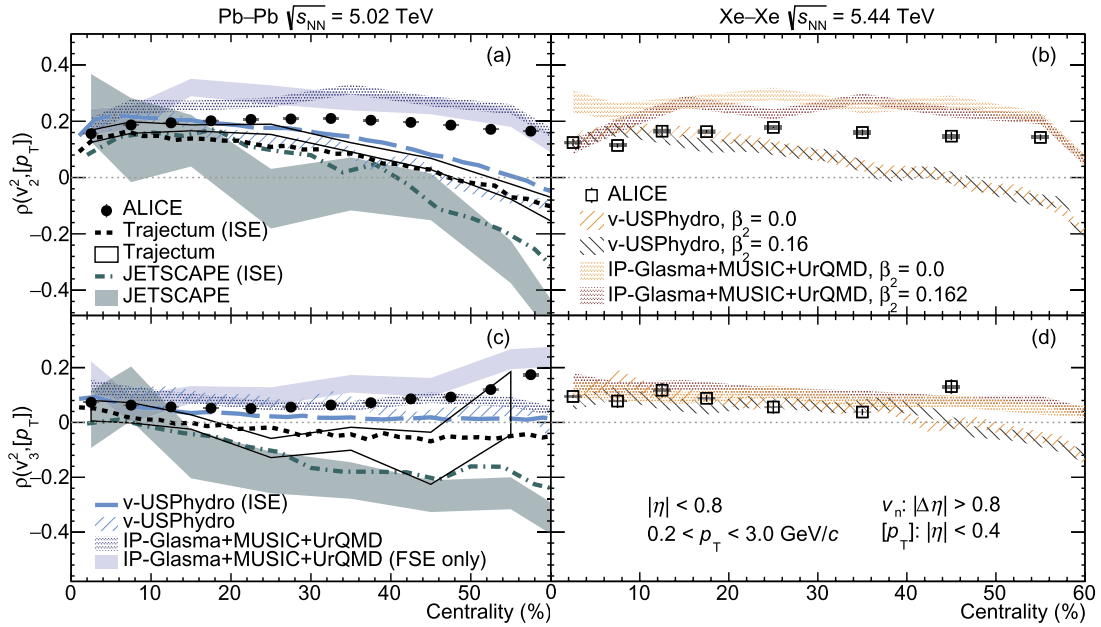


Fig. 1. Centrality dependence of $\rho(v_2^2, [p_T])$ (top) and $\rho(v_3^2, [p_T])$ (bottom) in Pb–Pb collisions at $\sqrt{s_{NN}} = 5.02$ TeV (a,c) and Xe–Xe collisions at $\sqrt{s_{NN}} = 5.44$ TeV (b, d). The statistical (systematic) uncertainties are shown as vertical bars (filled boxes). The initial-state estimations (ISE) are represented by lines, while IP-Glasma+MUSIC+UrQMD [31], v-USPhydro [45], Trajectum [35], and JETSCAPE [36] hydrodynamic model calculations are shown with hatched bands.

while any potential systematic uncertainty arising from different parametrizations of the models has not been evaluated. The v-USPhydro model uses T_RENTo initial conditions tuned in Ref. [63] and evolved by the v-USPhydro hydrodynamic code [45]. The Trajectum [35] and JETSCAPE [36] predictions are also based on T_RENTo initial conditions but as described in Refs. [35] and [36], respectively. The IP-Glasma+MUSIC+UrQMD model uses IP-Glasma initial conditions [64,65] followed by the MUSIC hydrodynamic model [66], coupled to a hadronic cascade model (UrQMD) [67,68]. In general, these models can quantitatively describe the previous measurements of particle p_T distributions and anisotropic flow [69,70]. As shown in Fig. 1, the IP-Glasma+MUSIC+UrQMD calculations capture the general trend of the measured $\rho(v_2^2, [p_T])$ with a weak centrality dependence, qualitatively describe the measurements in Pb–Pb and Xe–Xe collisions, but slightly overestimates the data. The v-USPhydro and Trajectum calculations exhibit a strong centrality dependence, underestimate the data by more than 50% for centrality above 30%, and have an opposite sign with respect to data for centralities above 40%. The discrepancies between the measurements and T_RENTo-based calculations become more pronounced with the JETSCAPE predictions [36], which become negative for semicentral collisions.

A recent study [71] showed that $\rho(v_2^2, [p_T])$ is more sensitive to the initial conditions of the collisions rather than to the transport properties of the QGP. This is also supported by the good agreement between the various hydrodynamic calculations and the correlation coefficients calculated directly from the corresponding initial-state model, which are presented by solid or dashed lines in the top panel of Fig. 1. These initial-state estimations (ISE) are calculated using the correlations of the energy of the fluid per unit rapidity at the initial time τ_0 and initial anisotropy coefficient ε_n [45]. Thus, differences between the calculations of $\rho(v_2^2, [p_T])$ shown in Fig. 1 are not primarily due to different hydrodynamic codes or treatments of hadronic interactions in these models. The different model predictions are rather caused by the difference in the initial energy density profile (geometric effect) and, potentially, a contribution from an initial momentum anisotropy, which is included in the IP-Glasma framework based on the CGC effective theory. The effect of initial momentum anisotropy is stud-

ied by comparing the hydrodynamic calculations using IP-Glasma initial conditions with and without initial momentum anisotropy (with only the final state effect labelled “FSE” shown by the light blue shadows). The IP-Glasma based calculations shown in Fig. 1 (a) are consistent with each other in the 0–60% Pb–Pb collisions. Thus, the different descriptions of ALICE data from IP-Glasma and T_RENTo based calculations are mainly driven by the initial geometric effects, which possibly originated from different values of ω parameter that determines the width of the colliding nucleus in the initial conditions [72]. The variable $\rho(v_2^2, [p_T])$ is the first observable for which such a significant difference is seen between T_RENTo and IP-Glasma models. Moreover, it is found that $\rho(v_2^2, [p_T])$ is sensitive to the quadrupole deformation parameter β_2 of deformed nuclei, such as ^{238}U or ^{129}Xe [46,73]. Previous flow measurements in Xe–Xe collisions [22] provided the estimation of $\beta_2 \approx 0.16$ for Xe using the data in the 0–5% central collisions. The $\rho(v_2^2, [p_T])$ calculation with $\beta_2 = 0$ and 0.162, based on IP-Glasma initial conditions in Fig. 1 (b), show a difference of 10–40% in the most central collisions. Comparisons of presented ALICE measurements to IP-Glasma+MUSIC+UrQMD calculations with the two different β_2 values suggest that the data agrees better with the IP-Glasma+MUSIC+UrQMD model calculations using $\beta_2 = 0.162$. Last but not least, the magnitude of $\rho(v_2^2, [p_T])$ measured in Pb–Pb collisions is larger than that in Xe–Xe collisions. Such a difference is predicted by both v-USPhydro and IP-Glasma+MUSIC+UrQMD calculations and is believed to be useful to discover a potential triaxial structure of ^{129}Xe at the LHC energies [74,75]. Comparisons with calculations that include different deformation scenarios could provide strong constraints on the ^{129}Xe nuclear structure. This is highly non-trivial because it is not entirely clear at the moment if the nuclear structure at the LHC energies, where the partonic degree of freedom is relevant, should be quantified by the same set of parameters as the low energy nuclear structure studies.

Fig. 1 (bottom) shows the centrality dependence of $\rho(v_3^2, [p_T])$ in the two colliding systems. The results are consistent within uncertainties for the considered centrality range. Both results show a positive value and rather a weak centrality dependence and a modest increase for centrality above 40% in Pb–Pb collisions. The IP-

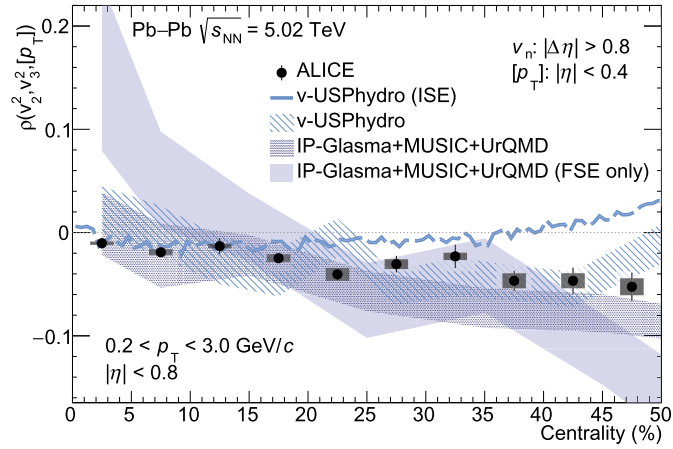


Fig. 2. Centrality dependence of $\rho(v_2^2, v_3^2, [p_T])$ in Pb–Pb collisions, shown by the solid circles. The statistical (systematic) uncertainties are shown as vertical bars (boxes). The initial-state estimations (ISE) as well as IP-Glasma+MUSIC+UrQMD [31] and v-USPhydro [45] hydrodynamic model calculations are compared with data.

Glasma+MUSIC+UrQMD calculations describe the presented ALICE measurements up to 50% centrality for Pb–Pb collisions, at which point they diverge from data with opposite trends for the full IP-Glasma+MUSIC+UrQMD calculation and the one with FSE only. It is unclear yet whether this difference between IP-Glasma+MUSIC+UrQMD calculation and the one with FSE can be attributed solely to the initial momentum anisotropy originating from the contributions of CGC in the IP-Glasma model, as only statistical uncertainties are considered in these calculations. In addition, both calculations describe the ALICE measurements from Xe–Xe collisions. The v-USPhydro calculations are roughly compatible with data in Pb–Pb collisions and are consistent with ALICE measurements up to 40% Xe–Xe collisions, then show a decreasing trend and become negative, which is not observed in the data. Like v-USPhydro, the Trajectory calculation is based on the $T_{\text{R}}\text{ENTo}$ initial state model but with a different tuning; it is negative for centrality above 10% and cannot describe the ALICE data in Pb–Pb collisions. It is also seen in Fig. 1 (bottom) that the $\rho(v_2^2, [p_T])$ calculations follow the trend of the initial-state estimations, which also show a significant difference and an opposite sign compared to the measurements. Such differences are further enhanced in the initial-state estimations from the JETSCAPE model, which does not consider the subnucleon structure. It is argued in a recent paper [76] that the positive $\rho(v_n^2, [p_T])$ for centrality up to 60% shown in Fig. 1 suggests a nucleon size of order 0.4–0.5 fm. This is much smaller than the values obtained from the recent Bayesian analyses [35,36]. Using $\rho(v_n^2, [p_T])$ measurements to constrain the width of nucleon is particularly interesting. It enables a new possibility to crosscheck different determinations of the nucleon and subnucleon scales relevant to inelastic processes at high energy in different experiments, e.g., in electron–ion collisions at the future Electron-Ion Collider.

In addition to $\rho(v_n^2, [p_T])$, a newly proposed higher-order correlation involving two flow coefficients, $\rho(v_n^2, v_m^2, [p_T])$ as defined in Eq. (3), is expected to bring further constraints on the initial-state shape [49]. Fig. 2 reports the first measurement of $\rho(v_2^2, v_3^2, [p_T])$ as a function of centrality up to 50% in Pb–Pb collisions at $\sqrt{s_{\text{NN}}} = 5.02$ TeV while the measurement in Xe–Xe collision is very challenging due to limited data sample. First of all, negative results are observed with more than 5σ significance from zero for the 0–50% centrality interval, showing a non-trivial anticorrelation between $[p_T]$, v_2 , and v_3 . It suggests an anticorrelation between entropy density, ε_2 , and ε_3 in the initial stage. The full IP-Glasma+MUSIC+UrQMD and v-USPhydro calculations presented in Fig. 2 show a flat trend with centrality as the ALICE data for the 0–40% cen-

trality range within uncertainties. As $\rho(v_2^2, v_3^2, [p_T])$ follows the trend of initial-state estimations and is mainly determined by the early stage [49], the differences among theoretical model calculations should again mainly originate from the initial conditions. Due to the large uncertainties of the model calculations, one cannot clearly establish a preference from comparisons with the ALICE data. Furthermore, the calculation of IP-Glasma with only the final state effect (FSE) shows a strong centrality dependence. It is positive in central collisions and gradually becomes negative in peripheral collisions. This trend is different from that of full IP-Glasma+MUSIC+UrQMD calculations and the experimental data.

In summary, the centrality dependence of correlations between anisotropic flow coefficients and mean transverse momentum in Pb–Pb and Xe–Xe collisions has been presented. These first ALICE measurements of $\rho(v_2^2, [p_T])$ and $\rho(v_3^2, [p_T])$ are found to be positive in both collision systems for the presented centrality ranges, confirming the positive correlations between v_2 (or v_3) and $[p_T]$. In addition, the higher-order correlation coefficient $\rho(v_2^2, v_3^2, [p_T])$ has been measured and found to be negative in Pb–Pb collisions, suggesting an anticorrelation between entropy density, initial anisotropy coefficients ε_2 and ε_3 in the initial stage. The experimental data reported in this Letter can be described by hydrodynamic models using IP-Glasma initial conditions, while they are not well reproduced by calculations using different tunings of the $T_{\text{R}}\text{ENTo}$ initial conditions. Such discrepancies cannot be attributed to the effect of the initial momentum anisotropy predicted by the CGC framework, as its impact is insignificant in the presented centrality ranges. Instead, the discrepancies are expected to arise from different geometric effects in the initial state. It should also be emphasized that the state-of-the-art extraction of the QGP’s transport coefficients relies on Bayesian analyses, which are all based on the $T_{\text{R}}\text{ENTo}$ model so far. The presented discrepancy between ALICE data and $T_{\text{R}}\text{ENTo}$ model-based calculations requires in-depth investigations, and the impact on the extraction of the properties of QGP should be explored further. The presented ALICE measurements are crucial on this matter, and including the presented data in the Bayesian global fitting could be a valuable step toward a better constraint on the initial state in nuclear collisions. Last but not least, the presented measurements in Xe–Xe collisions open a new window to study the nuclear structure using ultrarelativistic heavy-ion collisions at the LHC.

Declaration of competing interest

The authors declare that they have no known competing financial interests or personal relationships that could have appeared to influence the work reported in this paper.

Data availability

Data will be made available on request.

Acknowledgements

The ALICE Collaboration would like to thank Giuliano Giacalone (v-USPhydro), Chun Shen, Bjoern Schenke (IP-Glasma), Wilke van der Schee (Trajectory), Julia Velkovska, Andi Mankolli (JETSCAPE), Piotr Bozek (Glauber+MUSIC) for providing the latest predictions from the state-of-the-art models.

The ALICE Collaboration would like to thank all its engineers and technicians for their invaluable contributions to the construction of the experiment and the CERN accelerator teams for the outstanding performance of the LHC complex. The ALICE Collaboration gratefully acknowledges the resources and support provided by all Grid centres and the Worldwide LHC Computing Grid (WLCG) collaboration. The ALICE Collaboration acknowledges the

following funding agencies for their support in building and running the ALICE detector: A. I. Alikhanyan National Science Laboratory (Yerevan Physics Institute) Foundation (ANSL), State Committee of Science and World Federation of Scientists (WFS), Armenia; Austrian Academy of Sciences, Austrian Science Fund (FWF): [M 2467-N36] and Nationalstiftung für Forschung, Technologie und Entwicklung, Austria; Ministry of Communications and High Technologies, National Nuclear Research Center, Azerbaijan; Conselho Nacional de Desenvolvimento Científico e Tecnológico (CNPq), Financiadora de Estudos e Projetos (Finep), Fundação de Amparo à Pesquisa do Estado de São Paulo (FAPESP) and Universidade Federal do Rio Grande do Sul (UFRGS), Brazil; Ministry of Education of China (MOEC), Ministry of Science & Technology of China (MSTC) and National Natural Science Foundation of China (NSFC), China; Ministry of Science and Education and Croatian Science Foundation, Croatia; Centro de Aplicaciones Tecnológicas y Desarrollo Nuclear (CEADEN), Cubaenergía, Cuba; Ministry of Education, Youth and Sports of the Czech Republic, Czech Republic; The Danish Council for Independent Research | Natural Sciences, the Villum Fonden and Danish National Research Foundation (DNRF), Denmark; Helsinki Institute of Physics (HIP), Finland; Commissariat à l’Energie Atomique (CEA) and Institut National de Physique Nucléaire et de Physique des Particules (IN2P3) and Centre National de la Recherche Scientifique (CNRS), France; Bundesministerium für Bildung und Forschung (BMBF) and GSI Helmholtzzentrum für Schwerionenforschung GmbH, Germany; General Secretariat for Research and Technology, Ministry of Education, Research and Religions, Greece; National Research, Development and Innovation Office, Hungary; Department of Atomic Energy Government of India (DAE), Department of Science and Technology, Government of India (DST), University Grants Commission, Government of India (UGC) and Council of Scientific and Industrial Research (CSIR), India; Indonesian Institute of Sciences, Indonesia; Istituto Nazionale di Fisica Nucleare (INFN), Italy; Japanese Ministry of Education, Culture, Sports, Science and Technology (MEXT), Japan Society for the Promotion of Science (JSPS) KAKENHI and Japanese Ministry of Education, Culture, Sports, Science and Technology (MEXT) of Applied Science (IIST), Japan; Consejo Nacional de Ciencia (CONACYT) y Tecnología, through Fondo de Cooperación Internacional en Ciencia y Tecnología (FONCICYT) and Dirección General de Asuntos del Personal Académico (DGAPA), Mexico; Nederlandse Organisatie voor Wetenschappelijk Onderzoek (NWO), Netherlands; The Research Council of Norway, Norway; Commission on Science and Technology for Sustainable Development in the South (COMSATS), Pakistan; Pontificia Universidad Católica del Perú, Peru; Ministry of Education and Science, National Science Centre and WUT ID-UB, Poland; Korea Institute of Science and Technology Information and National Research Foundation of Korea (NRF), Republic of Korea; Ministry of Education and Scientific Research, Institute of Atomic Physics, Ministry of Research and Innovation and Institute of Atomic Physics and University Politehnica of Bucharest, Romania; Joint Institute for Nuclear Research (JINR), Ministry of Education and Science of the Russian Federation, National Research Centre Kurchatov Institute, Russian Science Foundation and Russian Foundation for Basic Research, Russia; Ministry of Education, Science, Research and Sport of the Slovak Republic, Slovakia; National Research Foundation of South Africa, South Africa; Swedish Research Council (VR) and Knut and Alice Wallenberg Foundation (KAW), Sweden; European Organization for Nuclear Research, Switzerland; Suranaree University of Technology (SUT), National Science and Technology Development Agency (NSDTA) and Office of the Higher Education Commission under NRU project of Thailand, Thailand; Turkish Energy, Nuclear and Mineral Research Agency (TENMAK), Turkey; National Academy of Sciences of Ukraine, Ukraine; Science and Technology Facilities Council (STFC), United Kingdom; National Science Foundation of the United States

of America (NSF) and United States Department of Energy, Office of Nuclear Physics (DOE NP), United States of America.

References

- [1] E.V. Shuryak, Quantum chromodynamics and the theory of superdense matter, *Phys. Rep.* 61 (1980) 71–158.
- [2] BRAHMS Collaboration, I. Arsene, et al., Quark gluon plasma and color glass condensate at RHIC? The perspective from the BRAHMS experiment, *Nucl. Phys. A* 757 (2005) 1–27, arXiv:nucl-ex/0410020.
- [3] PHENIX Collaboration, K. Adcox, et al., Formation of dense partonic matter in relativistic nucleus-nucleus collisions at RHIC: experimental evaluation by the PHENIX collaboration, *Nucl. Phys. A* 757 (2005) 184–283, arXiv:nucl-ex/0410003.
- [4] PHOBOS Collaboration, B.B. Back, et al., The PHOBOS perspective on discoveries at RHIC, *Nucl. Phys. A* 757 (2005) 28–101, arXiv:nucl-ex/0410022.
- [5] STAR Collaboration, J. Adams, et al., Experimental and theoretical challenges in the search for the quark gluon plasma: the STAR collaboration’s critical assessment of the evidence from RHIC collisions, *Nucl. Phys. A* 757 (2005) 102–183, arXiv:nucl-ex/0501009.
- [6] B. Muller, J. Schukraft, B. Wyslouch, First results from Pb+Pb collisions at the LHC, *Annu. Rev. Nucl. Part. Sci.* 62 (2012) 361–386, arXiv:1202.3233 [hep-ex].
- [7] G. Roland, K. Safarik, P. Steinberg, Heavy-ion collisions at the LHC, *Prog. Part. Nucl. Phys.* 77 (2014) 70–127.
- [8] J.-Y. Ollitrault, Anisotropy as a signature of transverse collective flow, *Phys. Rev. D* 46 (1992) 229–245.
- [9] S. Voloshin, Y. Zhang, Flow study in relativistic nuclear collisions by Fourier expansion of azimuthal particle distributions, *Z. Phys. C* 70 (1996) 665–672, arXiv:hep-ph/9407282 [hep-ph].
- [10] ALICE Collaboration, K. Aamodt, et al., Higher harmonic anisotropic flow measurements of charged particles in Pb–Pb collisions at $\sqrt{s_{NN}} = 2.76$ TeV, *Phys. Rev. Lett.* 107 (2011) 032301, arXiv:1105.3865 [nucl-ex].
- [11] ATLAS Collaboration, G. Aad, et al., Measurement of the azimuthal anisotropy for charged particle production in $\sqrt{s_{NN}} = 2.76$ TeV lead-lead collisions with the ATLAS detector, *Phys. Rev. C* 86 (2012) 014907, arXiv:1203.3087 [hep-ex].
- [12] CMS Collaboration, S. Chatrchyan, et al., Measurement of higher-order harmonic azimuthal anisotropy in PbPb collisions at $\sqrt{s_{NN}} = 2.76$ TeV, *Phys. Rev. C* 89 (4) (2014) 044906, arXiv:1310.8651 [nucl-ex].
- [13] ATLAS Collaboration, G. Aad, et al., Measurement of the distributions of event-by-event flow harmonics in lead-lead collisions $\sqrt{s_{NN}} = 2.76$ TeV with the ATLAS detector at the LHC, *J. High Energy Phys.* 11 (2013) 183, arXiv:1305.2942 [hep-ex].
- [14] ATLAS Collaboration, G. Aad, et al., Measurement of event-plane correlations in $\sqrt{s_{NN}} = 2.76$ TeV lead-lead collisions with the ATLAS detector, *Phys. Rev. C* 90 (2) (2014) 024905, arXiv:1403.0489 [hep-ex].
- [15] ATLAS Collaboration, G. Aad, et al., Measurement of the correlation between flow harmonics of different order in lead-lead collisions at $\sqrt{s_{NN}} = 2.76$ TeV with the ATLAS detector, *Phys. Rev. C* 92 (3) (2015) 034903, arXiv:1504.01289 [hep-ex].
- [16] ALICE Collaboration, J. Adam, et al., Correlated event-by-event fluctuations of flow harmonics in Pb–Pb collisions at $\sqrt{s_{NN}} = 2.76$ TeV, *Phys. Rev. Lett.* 117 (2016) 182301, arXiv:1604.07663 [nucl-ex].
- [17] ALICE Collaboration, J. Adam, et al., Anisotropic flow of charged particles in Pb–Pb collisions at $\sqrt{s_{NN}} = 5.02$ TeV, *Phys. Rev. Lett.* 116 (13) (2016) 132302, arXiv:1602.01119 [nucl-ex].
- [18] CMS Collaboration, A.M. Sirunyan, et al., Non-Gaussian elliptic-flow fluctuations in PbPb collisions at $\sqrt{s_{NN}} = 5.02$ TeV, *Phys. Lett. B* 789 (2019) 643–665, arXiv:1711.05594 [nucl-ex].
- [19] ALICE Collaboration, S. Acharya, et al., Searches for transverse momentum dependent flow vector fluctuations in Pb–Pb and p–Pb collisions at the LHC, *J. High Energy Phys.* 09 (2017) 032, arXiv:1707.05690 [nucl-ex].
- [20] ALICE Collaboration, S. Acharya, et al., Linear and non-linear flow modes in Pb–Pb collisions at $\sqrt{s_{NN}} = 2.76$ TeV, *Phys. Lett. B* 773 (2017) 68–80, arXiv:1705.04377 [nucl-ex].
- [21] ALICE Collaboration, S. Acharya, et al., Energy dependence and fluctuations of anisotropic flow in Pb–Pb collisions at $\sqrt{s_{NN}} = 5.02$ and 2.76 TeV, *J. High Energy Phys.* 07 (2018) 103, arXiv:1804.02944 [nucl-ex].
- [22] ALICE Collaboration, S. Acharya, et al., Anisotropic flow in Xe–Xe collisions at $\sqrt{s_{NN}} = 5.44$ TeV, *Phys. Lett. B* 784 (2018) 82–95, arXiv:1805.01832 [nucl-ex].
- [23] ALICE Collaboration, S. Acharya, et al., Non-linear flow modes of identified particles in Pb–Pb collisions at $\sqrt{s_{NN}} = 5.02$ TeV, *J. High Energy Phys.* 06 (2020) 147, arXiv:1912.00740 [nucl-ex].
- [24] ALICE Collaboration, S. Acharya, et al., Linear and non-linear flow modes of charged hadrons in Pb–Pb collisions at $\sqrt{s_{NN}} = 5.02$ TeV, *J. High Energy Phys.* 05 (2020) 085, arXiv:2002.00633 [nucl-ex].
- [25] ALICE Collaboration, S. Acharya, et al., Measurements of mixed harmonic cumulants in Pb–Pb collisions at $\sqrt{s_{NN}} = 5.02$ TeV, *Phys. Lett. B* 818 (2021) 136354, arXiv:2102.12180 [nucl-ex].
- [26] U. Heinz, R. Snellings, Collective flow and viscosity in relativistic heavy-ion collisions, *Annu. Rev. Nucl. Part. Sci.* 63 (2013) 123–151, arXiv:1301.2826 [nucl-th].

- [27] M. Luzum, H. Petersen, Initial state fluctuations and final state correlations in relativistic heavy-ion collisions, *J. Phys. G* 41 (2014) 063102, arXiv:1312.5503 [nucl-th].
- [28] E. Shuryak, Strongly coupled quark-gluon plasma in heavy ion collisions, *Rev. Mod. Phys.* 89 (2017) 035001, arXiv:1412.8393 [hep-ph].
- [29] H. Song, Y. Zhou, K. Gajdosova, Collective flow and hydrodynamics in large and small systems at the LHC, *Nucl. Sci. Tech.* 28 (7) (2017) 99, arXiv:1703.00670 [nucl-th].
- [30] G. Giacalone, F.G. Gardim, J. Noronha-Hostler, J.-Y. Ollitrault, Skewness of mean transverse momentum fluctuations in heavy-ion collisions, *Phys. Rev. C* 103 (2) (2021) 024910, arXiv:2004.09799 [nucl-th].
- [31] B. Schenke, C. Shen, D. Teaney, Transverse momentum fluctuations and their correlation with elliptic flow in nuclear collision, *Phys. Rev. C* 102 (3) (2020) 034905, arXiv:2004.00690 [nucl-th].
- [32] P. Božek, W. Broniowski, Transverse momentum fluctuations in ultrarelativistic Pb + Pb and p + Pb collisions with “wounded” quarks, *Phys. Rev. C* 96 (1) (2017) 014904, arXiv:1701.09105 [nucl-th].
- [33] J.E. Bernhard, J.S. Moreland, S.A. Bass, Bayesian estimation of the specific shear and bulk viscosity of quark-gluon plasma, *Nat. Phys.* 15 (11) (2019) 1113–1117.
- [34] JETSCAPE Collaboration, D. Everett, et al., Multisystem Bayesian constraints on the transport coefficients of QCD matter, *Phys. Rev. C* 103 (5) (2021) 054904, arXiv:2011.01430 [hep-ph].
- [35] G. Nijs, W. van der Schee, U. Gürsoy, R. Snellings, Transverse momentum differential global analysis of heavy-ion collisions, *Phys. Rev. Lett.* 126 (20) (2021) 202301, arXiv:2010.15130 [nucl-th].
- [36] JETSCAPE Collaboration, D. Everett, et al., Phenomenological constraints on the transport properties of QCD matter with data-driven model averaging, *Phys. Rev. Lett.* 126 (24) (2021) 242301, arXiv:2010.03928 [hep-ph].
- [37] P. Huovinen, P.F. Kolb, U.W. Heinz, P.V. Ruuskanen, S.A. Voloshin, Radial and elliptic flow at RHIC: further predictions, *Phys. Lett. B* 503 (2001) 58–64, arXiv:hep-ph/0101136.
- [38] D. Teaney, J. Lauret, E.V. Shuryak, Flow at the SPS and RHIC as a quark gluon plasma signature, *Phys. Rev. Lett.* 86 (2001) 4783–4786, arXiv:nucl-th/0011058.
- [39] ALICE Collaboration, J. Adam, et al., Event shape engineering for inclusive spectra and elliptic flow in Pb–Pb collisions at $\sqrt{s_{NN}} = 2.76$ TeV, *Phys. Rev. C* 93 (3) (2016) 034916, arXiv:1507.06194 [nucl-ex].
- [40] P. Bozek, Transverse-momentum–flow correlations in relativistic heavy-ion collisions, *Phys. Rev. C* 93 (4) (2016) 044908, arXiv:1601.04513 [nucl-th].
- [41] S.A. Voloshin, V. Koch, H.G. Ritter, Event-by-event fluctuations in collective quantities, *Phys. Rev. C* 60 (1999) 024901, arXiv:nucl-th/9903060.
- [42] ALICE Collaboration, B.B. Abelev, et al., Event-by-event mean p_T fluctuations in pp and Pb–Pb collisions at the LHC, *Eur. Phys. J. C* 74 (10) (2014) 3077, arXiv:1407.5530 [nucl-ex].
- [43] STAR Collaboration, J. Adam, et al., Collision-energy dependence of p_t correlations in Au + Au collisions at energies available at the BNL relativistic heavy ion collider, *Phys. Rev. C* 99 (4) (2019) 044918, arXiv:1901.00837 [nucl-ex].
- [44] G. Giacalone, B. Schenke, C. Shen, Observable signatures of initial state momentum anisotropies in nuclear collisions, *Phys. Rev. Lett.* 125 (19) (2020) 192301, arXiv:2006.15721 [nucl-th].
- [45] G. Giacalone, F.G. Gardim, J. Noronha-Hostler, J.-Y. Ollitrault, Correlation between mean transverse momentum and anisotropic flow in heavy-ion collisions, *Phys. Rev. C* 103 (2) (2021) 024909, arXiv:2004.01765 [nucl-th].
- [46] G. Giacalone, Constraining the quadrupole deformation of atomic nuclei with relativistic nuclear collisions, *Phys. Rev. C* 102 (2) (2020) 024901, arXiv:2004.14463 [nucl-th].
- [47] P. Möller, A.J. Sierk, T. Ichikawa, H. Sagawa, Nuclear ground-state masses and deformations: FRDM(2012), *At. Data Nucl. Data Tables* 109–110 (2016) 1–204, arXiv:1508.06294 [nucl-th].
- [48] ATLAS Collaboration, G. Aad, et al., Measurement of flow harmonics correlations with mean transverse momentum in lead-lead and proton-lead collisions at $\sqrt{s_{NN}} = 5.02$ TeV with the ATLAS detector, *Eur. Phys. J. C* 79 (12) (2019) 985, arXiv:1907.05176 [nucl-ex].
- [49] P. Božek, R. Samanta, Higher order cumulants of transverse momentum and harmonic flow in relativistic heavy ion collisions, arXiv:2103.15338 [nucl-th].
- [50] A. Bilandzic, C.H. Christensen, K. Gulbrandsen, A. Hansen, Y. Zhou, Generic framework for anisotropic flow analyses with multiparticle azimuthal correlations, *Phys. Rev. C* 89 (6) (2014) 064904, arXiv:1312.3572 [nucl-ex].
- [51] ALICE Collaboration, S. Acharya, et al., Systematic studies of correlations between different order flow harmonics in Pb–Pb collisions at $\sqrt{s_{NN}} = 2.76$ TeV, *Phys. Rev. C* 97 (2) (2018) 024906, arXiv:1709.01127 [nucl-ex].
- [52] Z. Moravcova, K. Gulbrandsen, Y. Zhou, Generic algorithm for multiparticle cumulants of azimuthal correlations in high energy nucleus collisions, *Phys. Rev. C* 103 (2) (2021) 024913, arXiv:2005.07974 [nucl-th].
- [53] E. Iancu, A. Leonidov, L.D. McLerran, Nonlinear gluon evolution in the color glass condensate. 1, *Nucl. Phys. A* 692 (2001) 583–645, arXiv:hep-ph/0011241.
- [54] E. Ferreiro, E. Iancu, A. Leonidov, L. McLerran, Nonlinear gluon evolution in the color glass condensate. 2, *Nucl. Phys. A* 703 (2002) 489–538, arXiv:hep-ph/0109115.
- [55] ALICE Collaboration, E. Abbas, et al., Performance of the ALICE VZERO system, *J. Instrum.* 8 (2013) P10016, arXiv:1306.3130 [nucl-ex].
- [56] ALICE Collaboration, J. Adam, et al., Centrality dependence of the charged-particle multiplicity density at midrapidity in Pb–Pb collisions at $\sqrt{s_{NN}} = 5.02$ TeV, *Phys. Rev. Lett.* 116 (22) (2016) 222302, arXiv:1512.06104 [nucl-ex].
- [57] ALICE Collaboration, B.B. Abelev, et al., Performance of the ALICE experiment at the CERN LHC, *Int. J. Mod. Phys. A* 29 (2014) 1430044, arXiv:1402.4476 [nucl-ex].
- [58] ALICE Collaboration, K. Aamodt, et al., Alignment of the ALICE Inner Tracking System with cosmic-ray tracks, *J. Instrum.* 5 (2010) P03003, arXiv:1001.0502 [physics.ins-det].
- [59] J. Alme, et al., The ALICE TPC, a large 3-dimensional tracking device with fast readout for ultra-high multiplicity events, *Nucl. Instrum. Methods A* 622 (2010) 316–367, arXiv:1001.1950 [physics.ins-det].
- [60] P. Huo, K. Gajdosov, J. Jia, Y. Zhou, Importance of non-flow in mixed-harmonic multi-particle correlations in small collision systems, *Phys. Lett. B* 777 (2018) 201–206, arXiv:1710.07567 [nucl-ex].
- [61] C. Zhang, A. Behera, S. Bhatta, J. Jia, Non-flow effects in correlation between harmonic flow and transverse momentum in nuclear collisions, *Phys. Lett. B* 822 (2021) 136702, arXiv:2102.05200 [nucl-th].
- [62] R. Barlow, Systematic errors: facts and fictions, in: *Conference on Advanced Statistical Techniques in Particle Physics* 7, 2002, pp. 134–144, arXiv:hep-ex/0207026.
- [63] J.E. Bernhard, J.S. Moreland, S.A. Bass, J. Liu, U. Heinz, Applying Bayesian parameter estimation to relativistic heavy-ion collisions: simultaneous characterization of the initial state and quark-gluon plasma medium, *Phys. Rev. C* 94 (2) (2016) 024907, arXiv:1605.03954 [hep-ph].
- [64] B. Schenke, P. Tribedy, R. Venugopalan, Event-by-event gluon multiplicity, energy density, and eccentricities in ultrarelativistic heavy-ion collisions, *Phys. Rev. C* 86 (2012) 034908, arXiv:1206.6805 [hep-ph].
- [65] B. Schenke, P. Tribedy, R. Venugopalan, Fluctuating glasma initial conditions and flow in heavy ion collisions, *Phys. Rev. Lett.* 108 (2012) 252301, arXiv:1202.6646 [nucl-th].
- [66] B. Schenke, S. Jeon, C. Gale, Elliptic and triangular flow in event-by-event (3+1) D viscous hydrodynamics, *Phys. Rev. Lett.* 106 (2011) 042301, arXiv:1009.3244 [hep-ph].
- [67] S.A. Bass, et al., Microscopic models for ultrarelativistic heavy ion collisions, *Prog. Part. Nucl. Phys.* 41 (1998) 255–369, arXiv:nucl-th/9803035 [nucl-th].
- [68] M. Bleicher, et al., Relativistic hadron-hadron collisions in the ultrarelativistic quantum molecular dynamics model, *J. Phys. G* 25 (1999) 1859–1896, arXiv:hep-ph/9909407 [hep-ph].
- [69] G. Giacalone, J. Noronha-Hostler, M. Luzum, J.-Y. Ollitrault, Hydrodynamic predictions for 5.44 TeV Xe+Xe collisions, *Phys. Rev. C* 97 (3) (2018) 034904, arXiv:1711.08499 [nucl-th].
- [70] S. McDonald, C. Shen, F. Fillion-Gourdeau, S. Jeon, C. Gale, Hydrodynamic predictions for Pb+Pb collisions at 5.02 TeV, *Phys. Rev. C* 95 (6) (2017) 064913, arXiv:1609.02958 [hep-ph].
- [71] N. Magdy, R.A. Lacey, Model investigations of the correlation between the mean transverse momentum and anisotropic flow in shape-engineered events, *Phys. Lett. B* 821 (2021) 136625, arXiv:2105.04879 [nucl-th].
- [72] J.S. Moreland, J.E. Bernhard, S.A. Bass, Alternative ansatz to wounded nucleon and binary collision scaling in high-energy nuclear collisions, *Phys. Rev. C* 92 (1) (2015) 011901, arXiv:1412.4708 [nucl-th].
- [73] G. Giacalone, Observing the deformation of nuclei with relativistic nuclear collisions, *Phys. Rev. Lett.* 124 (20) (2020) 202301, arXiv:1910.04673 [nucl-th].
- [74] B. Bally, M. Bender, G. Giacalone, V. Somà, Evidence of the triaxial structure of ^{129}Xe at the Large Hadron Collider, arXiv:2108.09578 [nucl-th].
- [75] J. Jia, Shape of atomic nuclei in heavy ion collisions, arXiv:2106.08768 [nucl-th].
- [76] G. Giacalone, B. Schenke, C. Shen, Constraining the nucleon size with relativistic nuclear collisions, *Phys. Rev. Lett.* 128 (4) (2022) 042301, arXiv:2111.02908 [nucl-th].

ALICE Collaboration

S. Acharya¹⁴³, D. Adamová⁹⁷, A. Adler⁷⁵, J. Adolfosson⁸², G. Aglieri Rinella³⁴, M. Agnello³⁰, N. Agrawal⁵⁴, Z. Ahammed¹⁴³, S. Ahmad¹⁶, S.U. Ahn⁷⁷, I. Ahuja³⁸, Z. Akbar⁵¹, A. Akhondinov⁹⁴, M. Al-Turany¹⁰⁹, S.N. Alam¹⁶, D. Aleksandrov⁹⁰, B. Alessandro⁶⁰, H.M. Alfanda⁷, R. Alfaro Molina⁷²,

B. Ali¹⁶, Y. Ali¹⁴, A. Alici²⁵, N. Alizadehvandchali¹²⁶, A. Alkin³⁴, J. Alme²¹, G. Alocco⁵⁵, T. Alt⁶⁹,
 I. Altsybeev¹¹⁴, M.N. Anaam⁷, C. Andrei⁴⁸, D. Andreou⁹², A. Andronic¹⁴⁶, M. Angeletti³⁴,
 V. Anguelov¹⁰⁶, F. Antinori⁵⁷, P. Antonioli⁵⁴, C. Anuj¹⁶, N. Apadula⁸¹, L. Aphecetche¹¹⁶,
 H. Appelshäuser⁶⁹, S. Arcelli²⁵, R. Arnaldi⁶⁰, I.C. Arsene²⁰, M. Arslandok¹⁴⁸, A. Augustinus³⁴,
 R. Averbeck¹⁰⁹, S. Aziz⁷⁹, M.D. Azmi¹⁶, A. Badalà⁵⁶, Y.W. Baek⁴¹, X. Bai^{130,109}, R. Bailhache⁶⁹,
 Y. Bailung⁵⁰, R. Bala¹⁰³, A. Balbino³⁰, A. Baldisseri¹⁴⁰, B. Balis², D. Banerjee⁴, Z. Banoo¹⁰³,
 R. Barbera²⁶, L. Barioglio¹⁰⁷, M. Barlou⁸⁶, G.G. Barnaföldi¹⁴⁷, L.S. Barnby⁹⁶, V. Barret¹³⁷, C. Bartels¹²⁹,
 K. Barth³⁴, E. Bartsch⁶⁹, F. Baruffaldi²⁷, N. Bastid¹³⁷, S. Basu⁸², G. Batigne¹¹⁶, B. Batyunya⁷⁶,
 D. Bauri⁴⁹, J.L. Bazo Alba¹¹³, I.G. Bearden⁹¹, C. Beattie¹⁴⁸, P. Becht¹⁰⁹, I. Belikov¹³⁹,
 A.D.C. Bell Hechavarria¹⁴⁶, F. Bellini²⁵, R. Bellwied¹²⁶, S. Belokurova¹¹⁴, V. Belyaev⁹⁵, G. Bencedi^{147,70},
 S. Beole²⁴, A. Bercuci⁴⁸, Y. Berdnikov¹⁰⁰, A. Berdnikova¹⁰⁶, L. Bergmann¹⁰⁶, M.G. Besoiu⁶⁸, L. Betev³⁴,
 P.P. Bhaduri¹⁴³, A. Bhasin¹⁰³, I.R. Bhat¹⁰³, M.A. Bhat⁴, B. Bhattacharjee⁴², P. Bhattacharya²²,
 L. Bianchi²⁴, N. Bianchi⁵², J. Bielčik³⁷, J. Bielčíková⁹⁷, J. Biernat¹¹⁹, A. Bilandzic¹⁰⁷, G. Biro¹⁴⁷,
 S. Biswas⁴, J.T. Blair¹²⁰, D. Blau^{90,83}, M.B. Blidaru¹⁰⁹, C. Blume⁶⁹, G. Boca^{28,58}, F. Bock⁹⁸,
 A. Bogdanov⁹⁵, S. Boi²², J. Bok⁶², L. Boldizsár¹⁴⁷, A. Bolozdynya⁹⁵, M. Bombara³⁸, P.M. Bond³⁴,
 G. Bonomi^{142,58}, H. Borel¹⁴⁰, A. Borissov⁸³, H. Bossi¹⁴⁸, E. Botta²⁴, L. Bratrud⁶⁹, P. Braun-Munzinger¹⁰⁹,
 M. Bregant¹²², M. Broz³⁷, G.E. Bruno^{108,33}, M.D. Buckland^{23,129}, D. Budnikov¹¹⁰, H. Buesching⁶⁹,
 S. Bufalino³⁰, O. Bugnon¹¹⁶, P. Buhler¹¹⁵, Z. Buthelezi^{73,133}, J.B. Butt¹⁴, A. Bylinkin¹²⁸, S.A. Bysiak¹¹⁹,
 M. Cai^{27,7}, H. Caines¹⁴⁸, A. Caliva¹⁰⁹, E. Calvo Villar¹¹³, J.M.M. Camacho¹²¹, R.S. Camacho⁴⁵,
 P. Camerini²³, F.D.M. Canedo¹²², F. Carnesecchi^{34,25}, R. Caron¹⁴⁰, J. Castillo Castellanos¹⁴⁰,
 E.A.R. Casula²², F. Catalano³⁰, C. Ceballos Sanchez⁷⁶, P. Chakraborty⁴⁹, S. Chandra¹⁴³, S. Chapeland³⁴,
 M. Chartier¹²⁹, S. Chattopadhyay¹⁴³, S. Chattopadhyay¹¹¹, T.G. Chavez⁴⁵, T. Cheng⁷, C. Cheshkov¹³⁸,
 B. Cheynis¹³⁸, V. Chibante Barroso³⁴, D.D. Chinellato¹²³, S. Cho⁶², P. Chochula³⁴, P. Christakoglou⁹²,
 C.H. Christensen⁹¹, P. Christiansen⁸², T. Chujo¹³⁵, C. Cicalo⁵⁵, L. Cifarelli²⁵, F. Cindolo⁵⁴,
 M.R. Ciupek¹⁰⁹, G. Clai^{54,II}, J. Cleymans^{125,I}, F. Colamaria⁵³, J.S. Colburn¹¹², D. Colella^{53,108,33},
 A. Collu⁸¹, M. Colocci³⁴, M. Concas^{60,III}, G. Conesa Balbastre⁸⁰, Z. Conesa del Valle⁷⁹, G. Contin²³,
 J.G. Contreras³⁷, M.L. Coquet¹⁴⁰, T.M. Cormier⁹⁸, P. Cortese³¹, M.R. Cosentino¹²⁴, F. Costa³⁴,
 S. Costanza^{28,58}, P. Crochet¹³⁷, R. Cruz-Torres⁸¹, E. Cuautle⁷⁰, P. Cui⁷, L. Cunqueiro⁹⁸, A. Dainese⁵⁷,
 M.C. Danisch¹⁰⁶, A. Danu⁶⁸, P. Das⁸⁸, P. Das⁴, S. Das⁴, S. Dash⁴⁹, A. De Caro²⁹, G. de Cataldo⁵³,
 L. De Cilladi²⁴, J. de Cuveland³⁹, A. De Falco²², D. De Gruttola²⁹, N. De Marco⁶⁰, C. De Martin²³,
 S. De Pasquale²⁹, S. Deb⁵⁰, H.F. Degenhardt¹²², K.R. Deja¹⁴⁴, R. Del Grande¹⁰⁷, L. Dello Stritto²⁹,
 W. Deng⁷, P. Dhankher¹⁹, D. Di Bari³³, A. Di Mauro³⁴, R.A. Diaz⁸, T. Dietel¹²⁵, Y. Ding^{138,7}, R. Divià³⁴,
 D.U. Dixit¹⁹, Ø. Djuvsland²¹, U. Dmitrieva⁶⁴, J. Do⁶², A. Dobrin⁶⁸, B. Dönigus⁶⁹, A.K. Dubey¹⁴³,
 A. Dubla^{109,92}, S. Dudi¹⁰², P. Dupieux¹³⁷, N. Dzalaiova¹³, T.M. Eder¹⁴⁶, R.J. Ehlers⁹⁸, V.N. Eikeland²¹,
 F. Eisenhut⁶⁹, D. Elia⁵³, B. Erazmus¹¹⁶, F. Ercolessi²⁵, F. Erhardt¹⁰¹, A. Erokhin¹¹⁴, M.R. Ersdal²¹,
 B. Espagnon⁷⁹, G. Eulisse³⁴, D. Evans¹¹², S. Evdokimov⁹³, L. Fabbietti¹⁰⁷, M. Faggin²⁷, J. Faivre⁸⁰,
 F. Fan⁷, A. Fantoni⁵², M. Fasel⁹⁸, P. Fedichio³⁰, A. Feliciello⁶⁰, G. Feofilov¹¹⁴, A. Fernández Téllez⁴⁵,
 A. Ferrero¹⁴⁰, A. Ferretti²⁴, V.J.G. Feuillard¹⁰⁶, J. Figiel¹¹⁹, V. Filova³⁷, D. Finogeev⁶⁴, F.M. Fionda⁵⁵,
 G. Fiorenza^{34,108}, F. Flor¹²⁶, A.N. Flores¹²⁰, S. Foertsch⁷³, S. Fokin⁹⁰, E. Fragiaco⁶¹, E. Frajna¹⁴⁷,
 A. Francisco¹³⁷, U. Fuchs³⁴, N. Funicello²⁹, C. Furget⁸⁰, A. Furs⁶⁴, J.J. Gaardhøje⁹¹, M. Gagliardi²⁴,
 A.M. Gago¹¹³, A. Gal¹³⁹, C.D. Galvan¹²¹, D.R. Gangadharan¹²⁶, P. Ganoti⁸⁶, C. Garabatos¹⁰⁹,
 J.R.A. Garcia⁴⁵, E. Garcia-Solis¹⁰, K. Garg¹¹⁶, C. Gargiulo³⁴, A. Garibli⁸⁹, K. Garner¹⁴⁶, P. Gasik¹⁰⁹,
 E.F. Gauger¹²⁰, A. Gautam¹²⁸, M.B. Gay Ducati⁷¹, M. Germain¹¹⁶, P. Ghosh¹⁴³, S.K. Ghosh⁴,
 M. Giacalone²⁵, P. Gianotti⁵², P. Giubellino^{109,60}, P. Giubileo²⁷, A.M.C. Glaenger¹⁴⁰, P. Glässel¹⁰⁶,
 E. Glimos¹³², D.J.Q. Goh⁸⁴, V. Gonzalez¹⁴⁵, L.H. González-Trueba⁷², S. Gorbunov³⁹, M. Gorgon²,
 L. Görlich¹¹⁹, S. Gotovac³⁵, V. Grabski⁷², L.K. Graczykowski¹⁴⁴, L. Greiner⁸¹, A. Grelli⁶³, C. Grigoras³⁴,
 V. Grigoriev⁹⁵, S. Grigoryan^{76,1}, F. Grosa^{34,60}, J.F. Grosse-Oetringhaus³⁴, R. Grosso¹⁰⁹, D. Grund³⁷,
 G.G. Guardiano¹²³, R. Guernane⁸⁰, M. Guilbaud¹¹⁶, K. Gulbrandsen⁹¹, T. Gunji¹³⁴, W. Guo⁷,
 A. Gupta¹⁰³, R. Gupta¹⁰³, S.P. Guzman⁴⁵, L. Gyulai¹⁴⁷, M.K. Habib¹⁰⁹, C. Hadjidakis⁷⁹, H. Hamagaki⁸⁴,
 M. Hamid⁷, R. Hannigan¹²⁰, M.R. Haque¹⁴⁴, A. Harlenderova¹⁰⁹, J.W. Harris¹⁴⁸, A. Harton¹⁰,
 J.A. Hasenbichler³⁴, H. Hassan⁹⁸, D. Hatzifotiadou⁵⁴, P. Hauer⁴³, L.B. Havener¹⁴⁸, S.T. Heckel¹⁰⁷,
 E. Hellbär¹⁰⁹, H. Helstrup³⁶, T. Herman³⁷, E.G. Hernandez⁴⁵, G. Herrera Corral⁹, F. Herrmann¹⁴⁶,
 K.F. Hetland³⁶, H. Hillemanns³⁴, C. Hills¹²⁹, B. Hippolyte¹³⁹, B. Hofman⁶³, B. Hohlweger⁹²,

J. Honermann¹⁴⁶, G.H. Hong¹⁴⁹, D. Horak³⁷, S. Hornung¹⁰⁹, A. Horzyk², R. Hosokawa¹⁵, Y. Hou⁷, P. Hristov³⁴, C. Hughes¹³², P. Huhn⁶⁹, L.M. Huhta¹²⁷, C.V. Hulse⁷⁹, T.J. Humanic⁹⁹, H. Hushnud¹¹¹, L.A. Husova¹⁴⁶, A. Hutson¹²⁶, J.P. Iddon^{34,129}, R. Ilkaev¹¹⁰, H. Ilyas¹⁴, M. Inaba¹³⁵, G.M. Innocenti³⁴, M. Ippolitov⁹⁰, A. Isakov⁹⁷, T. Isidori¹²⁸, M.S. Islam¹¹¹, M. Ivanov¹⁰⁹, V. Ivanov¹⁰⁰, V. Izucheev⁹³, M. Jablonski², B. Jacak⁸¹, N. Jacazio³⁴, P.M. Jacobs⁸¹, S. Jadlovská¹¹⁸, J. Jadlovsky¹¹⁸, S. Jaelani⁶³, C. Jahnke^{123,122}, M.J. Jakubowska¹⁴⁴, A. Jaloitra¹⁰³, M.A. Janik¹⁴⁴, T. Janson⁷⁵, M. Jercic¹⁰¹, O. Jevons¹¹², A.A.P. Jimenez⁷⁰, F. Jonas^{98,146}, P.G. Jones¹¹², J.M. Jowett^{34,109}, J. Jung⁶⁹, M. Jung⁶⁹, A. Junique³⁴, A. Jusko¹¹², M.J. Kabus¹⁴⁴, J. Kaewjai¹¹⁷, P. Kalinak⁶⁵, A.S. Kalteyer¹⁰⁹, A. Kalweit³⁴, V. Kaplin⁹⁵, A. Karasu Uysal⁷⁸, D. Karatovic¹⁰¹, O. Karavichev⁶⁴, T. Karavicheva⁶⁴, P. Karczmarczyk¹⁴⁴, E. Karpechev⁶⁴, V. Kashyap⁸⁸, A. Kazantsev⁹⁰, U. Keschull⁷⁵, R. Keidel⁴⁷, D.L.D. Keijdener⁶³, M. Keil³⁴, B. Ketzer⁴³, Z. Khabanova⁹², A.M. Khan⁷, S. Khan¹⁶, A. Khanzadeev¹⁰⁰, Y. Kharlov^{93,83}, A. Khatun¹⁶, A. Khuntia¹¹⁹, B. Kileng³⁶, B. Kim^{17,62}, C. Kim¹⁷, D.J. Kim¹²⁷, E.J. Kim⁷⁴, J. Kim¹⁴⁹, J.S. Kim⁴¹, J. Kim¹⁰⁶, J. Kim⁷⁴, M. Kim¹⁰⁶, S. Kim¹⁸, T. Kim¹⁴⁹, S. Kirsch⁶⁹, I. Kisel³⁹, S. Kiselev⁹⁴, A. Kisiel¹⁴⁴, J.P. Kitowski², J.L. Klay⁶, J. Klein³⁴, S. Klein⁸¹, C. Klein-Bösing¹⁴⁶, M. Kleiner⁶⁹, T. Klemenz¹⁰⁷, A. Kluge³⁴, A.G. Knospe¹²⁶, C. Kobdaj¹¹⁷, T. Kollegger¹⁰⁹, A. Kondratyev⁷⁶, N. Kondratyeva⁹⁵, E. Kondratyuk⁹³, J. König⁶⁹, S.A. Königstorfer¹⁰⁷, P.J. Konopka³⁴, G. Kornakov¹⁴⁴, S.D. Koryciak², A. Kotliarov⁹⁷, O. Kovalenko⁸⁷, V. Kovalenko¹¹⁴, M. Kowalski¹¹⁹, I. Králik⁶⁵, A. Kravčáková³⁸, L. Kreis¹⁰⁹, M. Krivda^{112,65}, F. Krizek⁹⁷, K. Krizkova Gajdosova³⁷, M. Kroesen¹⁰⁶, M. Krüger⁶⁹, D.M. Krupova³⁷, E. Kryshen¹⁰⁰, M. Krzewicki³⁹, V. Kučera³⁴, C. Kuhn¹³⁹, P.G. Kuijter⁹², T. Kumaoka¹³⁵, D. Kumar¹⁴³, L. Kumar¹⁰², N. Kumar¹⁰², S. Kundu³⁴, P. Kurashvili⁸⁷, A. Kurepin⁶⁴, A.B. Kurepin⁶⁴, A. Kuryakin¹¹⁰, S. Kushpil⁹⁷, J. Kvapil¹¹², M.J. Kweon⁶², J.Y. Kwon⁶², Y. Kwon¹⁴⁹, S.L. La Pointe³⁹, P. La Rocca²⁶, Y.S. Lai⁸¹, A. Lakrathok¹¹⁷, M. Lamanna³⁴, R. Langoy¹³¹, K. Lapidus³⁴, P. Larionov^{34,52}, E. Laudi³⁴, L. Lautner^{34,107}, R. Lavicka^{115,37}, T. Lazareva¹¹⁴, R. Lea^{142,23,58}, J. Lehrbach³⁹, R.C. Lemmon⁹⁶, I. León Monzón¹²¹, E.D. Lesser¹⁹, M. Lettrich^{34,107}, P. Lévai¹⁴⁷, X. Li¹¹, X.L. Li⁷, J. Lien¹³¹, R. Lietava¹¹², B. Lim¹⁷, S.H. Lim¹⁷, V. Lindenstruth³⁹, A. Lindner⁴⁸, C. Lippmann¹⁰⁹, A. Liu¹⁹, D.H. Liu⁷, J. Liu¹²⁹, I.M. Lofnes²¹, V. Loginov⁹⁵, C. Loizides⁹⁸, P. Loncar³⁵, J.A. Lopez¹⁰⁶, X. Lopez¹³⁷, E. López Torres⁸, J.R. Luhder¹⁴⁶, M. Lunardon²⁷, G. Luparello⁶¹, Y.G. Ma⁴⁰, A. Maevskaya⁶⁴, M. Mager³⁴, T. Mahmoud⁴³, A. Maire¹³⁹, M. Malaev¹⁰⁰, N.M. Malik¹⁰³, Q.W. Malik²⁰, S.K. Malik¹⁰³, L. Malinina^{76,IV}, D. Mal'Kevich⁹⁴, D. Mallick⁸⁸, N. Mallick⁵⁰, G. Mandaglio^{32,56}, V. Manko⁹⁰, F. Manso¹³⁷, V. Manzari⁵³, Y. Mao⁷, G.V. Margagliotti²³, A. Margotti⁵⁴, A. Marín¹⁰⁹, C. Markert¹²⁰, M. Marquard⁶⁹, N.A. Martin¹⁰⁶, P. Martinengo³⁴, J.L. Martinez¹²⁶, M.I. Martínez⁴⁵, G. Martínez García¹¹⁶, S. Masciocchi¹⁰⁹, M. Maserà²⁴, A. Masoni⁵⁵, L. Massacrier⁷⁹, A. Mastroserio^{141,53}, A.M. Mathis¹⁰⁷, O. Matonoha⁸², P.F.T. Matuoka¹²², A. Matyja¹¹⁹, C. Mayer¹¹⁹, A.L. Mazuecos³⁴, F. Mazzaschi²⁴, M. Mazzilli³⁴, M.A. Mazzoni^{59,1}, J.E. Mdhuli¹³³, A.F. Mechler⁶⁹, Y. Melikyan⁶⁴, A. Menchaca-Rocha⁷², E. Meninno^{115,29}, A.S. Menon¹²⁶, M. Meres¹³, S. Mhlanga^{125,73}, Y. Miake¹³⁵, L. Micheletti⁶⁰, L.C. Migliorin¹³⁸, D.L. Mihaylov¹⁰⁷, K. Mikhaylov^{76,94}, A.N. Mishra¹⁴⁷, D. Miśkowiec¹⁰⁹, A. Modak⁴, A.P. Mohanty⁶³, B. Mohanty⁸⁸, M. Mohisin Khan^{16,V}, M.A. Molander⁴⁴, Z. Moravcova⁹¹, C. Mordasini¹⁰⁷, D.A. Moreira De Godoy¹⁴⁶, I. Morozov⁶⁴, A. Morsch³⁴, T. Mrnjavac³⁴, V. Muccifora⁵², E. Mudnic³⁵, D. Mühlheim¹⁴⁶, S. Muhuri¹⁴³, J.D. Mulligan⁸¹, A. Mulliri²², M.G. Munhoz¹²², R.H. Munzer⁶⁹, H. Murakami¹³⁴, S. Murray¹²⁵, L. Musa³⁴, J. Musinsky⁶⁵, J.W. Myrcha¹⁴⁴, B. Naik¹³³, R. Nair⁸⁷, B.K. Nandi⁴⁹, R. Nania⁵⁴, E. Nappi⁵³, A.F. Nassirpour⁸², A. Nath¹⁰⁶, C. Nattrass¹³², A. Neagu²⁰, A. Negru¹³⁶, L. Nellen⁷⁰, S.V. Nesbo³⁶, G. Neskovic³⁹, D. Nesterov¹¹⁴, B.S. Nielsen⁹¹, E.G. Nielsen⁹¹, S. Nikolaev⁹⁰, S. Nikulin⁹⁰, V. Nikulin¹⁰⁰, F. Noferini⁵⁴, S. Noh¹², P. Nomokonov⁷⁶, J. Norman¹²⁹, N. Novitzky¹³⁵, P. Nowakowski¹⁴⁴, A. Nyanin⁹⁰, J. Nystrand²¹, M. Ogino⁸⁴, A. Ohlson⁸², V.A. Okorokov⁹⁵, J. Oleniacz¹⁴⁴, A.C. Oliveira Da Silva¹³², M.H. Oliver¹⁴⁸, A. Onnerstad¹²⁷, C. Oppedisano⁶⁰, A. Ortiz Velasquez⁷⁰, T. Osako⁴⁶, A. Oskarsson⁸², J. Otwinowski¹¹⁹, M. Oya⁴⁶, K. Oyama⁸⁴, Y. Pachmayer¹⁰⁶, S. Padhan⁴⁹, D. Pagano^{142,58}, G. Paić⁷⁰, A. Palasciano⁵³, J. Pan¹⁴⁵, S. Panebianco¹⁴⁰, J. Park⁶², J.E. Parkkila¹²⁷, S.P. Pathak¹²⁶, R.N. Patra^{103,34}, B. Paul²², H. Pei⁷, T. Peitzmann⁶³, X. Peng⁷, L.G. Pereira⁷¹, H. Pereira Da Costa¹⁴⁰, D. Peresunko^{90,83}, G.M. Perez⁸, S. Perrin¹⁴⁰, Y. Pestov⁵, V. Petráček³⁷, M. Petrovici⁴⁸, R.P. Pezzi^{116,71}, S. Piano⁶¹, M. Pikna¹³, P. Pillot¹¹⁶, O. Pinazza^{54,34}, L. Pinsky¹²⁶, C. Pinto²⁶, S. Pisano⁵², M. Płoskoń⁸¹, M. Planinic¹⁰¹, F. Pliquett⁶⁹, M.G. Poghosyan⁹⁸, B. Polichtchouk⁹³, S. Politano³⁰, N. Poljak¹⁰¹, A. Pop⁴⁸, S. Porteboeuf-Houssais¹³⁷, J. Porter⁸¹, V. Pozdniakov⁷⁶, S.K. Prasad⁴, R. Preghenella⁵⁴, F. Prino⁶⁰,

C.A. Pruneau¹⁴⁵, I. Pshenichnov⁶⁴, M. Puccio³⁴, S. Qiu⁹², L. Quaglia²⁴, R.E. Quishpe¹²⁶, S. Ragoni¹¹², A. Rakotozafindrabe¹⁴⁰, L. Ramello³¹, F. Rami¹³⁹, S.A.R. Ramirez⁴⁵, A.G.T. Ramos³³, T.A. Rancien⁸⁰, R. Raniwala¹⁰⁴, S. Raniwala¹⁰⁴, S.S. Räsänen⁴⁴, R. Rath⁵⁰, I. Ravasenga⁹², K.F. Read^{98,132}, A.R. Redelbach³⁹, K. Redlich^{87,VI}, A. Rehman²¹, P. Reichelt⁶⁹, F. Reidt³⁴, H.A. Reme-ness³⁶, Z. Rescakova³⁸, K. Reygers¹⁰⁶, A. Riabov¹⁰⁰, V. Riabov¹⁰⁰, T. Richert⁸², M. Richter²⁰, W. Riegler³⁴, F. Riggi²⁶, C. Ristea⁶⁸, M. Rodríguez Cahuantzi⁴⁵, K. Røed²⁰, R. Rogalev⁹³, E. Rogochaya⁷⁶, T.S. Rogoschinski⁶⁹, D. Rohr³⁴, D. Röhrich²¹, P.F. Rojas⁴⁵, S. Rojas Torres³⁷, P.S. Rokita¹⁴⁴, F. Ronchetti⁵², A. Rosano^{32,56}, E.D. Rosas⁷⁰, A. Rossi⁵⁷, A. Roy⁵⁰, P. Roy¹¹¹, S. Roy⁴⁹, N. Rubini²⁵, O.V. Rueda⁸², D. Ruggiano¹⁴⁴, R. Rui²³, B. Rumyantsev⁷⁶, P.G. Russek², R. Russo⁹², A. Rustamov⁸⁹, E. Ryabinkin⁹⁰, Y. Ryabov¹⁰⁰, A. Rybicki¹¹⁹, H. Rytönen¹²⁷, W. Rzesza¹⁴⁴, O.A.M. Saarimaki⁴⁴, R. Sadek¹¹⁶, S. Sadovsky⁹³, J. Saetre²¹, K. Šafařík³⁷, S.K. Saha¹⁴³, S. Saha⁸⁸, B. Sahoo⁴⁹, P. Sahoo⁴⁹, R. Sahoo⁵⁰, S. Sahoo⁶⁶, D. Sahu⁵⁰, P.K. Sahu⁶⁶, J. Saini¹⁴³, S. Sakai¹³⁵, M.P. Salvan¹⁰⁹, S. Sambyal¹⁰³, V. Samsonov^{100,95,I}, T.B. Saramela¹²², D. Sarkar¹⁴⁵, N. Sarkar¹⁴³, P. Sarma⁴², V.M. Sarti¹⁰⁷, M.H.P. Sas¹⁴⁸, J. Schambach⁹⁸, H.S. Scheid⁶⁹, C. Schiaua⁴⁸, R. Schicker¹⁰⁶, A. Schmah¹⁰⁶, C. Schmidt¹⁰⁹, H.R. Schmidt¹⁰⁵, M.O. Schmidt^{34,106}, M. Schmidt¹⁰⁵, N.V. Schmidt^{98,69}, A.R. Schmier¹³², R. Schotter¹³⁹, J. Schukraft³⁴, K. Schwarz¹⁰⁹, K. Schweda¹⁰⁹, G. Scioli²⁵, E. Scapparini⁶⁰, J.E. Seger¹⁵, Y. Sekiguchi¹³⁴, D. Sekihata¹³⁴, I. Selyuzhenkov^{109,95}, S. Senyukov¹³⁹, J.J. Seo⁶², D. Serebryakov⁶⁴, L. Šerkšnytė¹⁰⁷, A. Sevcenco⁶⁸, T.J. Shaba⁷³, A. Shabanov⁶⁴, A. Shabetai¹¹⁶, R. Shahoyan³⁴, W. Shaikh¹¹¹, A. Shangaraev⁹³, A. Sharma¹⁰², H. Sharma¹¹⁹, M. Sharma¹⁰³, N. Sharma¹⁰², S. Sharma¹⁰³, U. Sharma¹⁰³, A. Shatat⁷⁹, O. Sheibani¹²⁶, K. Shigaki⁴⁶, M. Shimomura⁸⁵, S. Shirinkin⁹⁴, Q. Shou⁴⁰, Y. Sibiriak⁹⁰, S. Siddhanta⁵⁵, T. Siemiarczuk⁸⁷, T.F. Silva¹²², D. Silvermyr⁸², T. Simantathammakul¹¹⁷, G. Simonetti³⁴, B. Singh¹⁰⁷, R. Singh⁸⁸, R. Singh¹⁰³, R. Singh⁵⁰, V.K. Singh¹⁴³, V. Singhal¹⁴³, T. Sinha¹¹¹, B. Sitar¹³, M. Sitta³¹, T.B. Skaali²⁰, G. Skorodumovs¹⁰⁶, M. Slupecki⁴⁴, N. Smirnov¹⁴⁸, R.J.M. Snellings⁶³, C. Soncco¹¹³, J. Song¹²⁶, A. Songmoolnak¹¹⁷, F. Soramel²⁷, S. Sorensen¹³², I. Sputowska¹¹⁹, J. Stachel¹⁰⁶, I. Stan⁶⁸, P.J. Steffanic¹³², S.F. Stiefelmaier¹⁰⁶, D. Stocco¹¹⁶, I. Storehaug²⁰, M.M. Støretvedt³⁶, P. Stratmann¹⁴⁶, C.P. Stylianidis⁹², A.A.P. Suaide¹²², C. Suire⁷⁹, M. Sukhanov⁶⁴, M. Suljic³⁴, R. Sultanov⁹⁴, V. Sumberia¹⁰³, S. Sumowidagdo⁵¹, S. Swain⁶⁶, A. Szabo¹³, I. Szarka¹³, U. Tabassam¹⁴, S.F. Taghavi¹⁰⁷, G. Taillepied¹³⁷, J. Takahashi¹²³, G.J. Tambave²¹, S. Tang^{137,7}, Z. Tang¹³⁰, J.D. Tapia Takaki^{128,VII}, M. Tarhini¹¹⁶, M.G. Tarzila⁴⁸, A. Tauro³⁴, G. Tejeda Muñoz⁴⁵, A. Telesca³⁴, L. Terlizzi²⁴, C. Terrevoli¹²⁶, G. Tersimonov³, S. Thakur¹⁴³, D. Thomas¹²⁰, R. Tieulent¹³⁸, A. Tikhonov⁶⁴, A.R. Timmins¹²⁶, M. Tkacik¹¹⁸, A. Toia⁶⁹, N. Topilskaya⁶⁴, M. Toppi⁵², F. Torales-Acosta¹⁹, T. Tork⁷⁹, A. Trifiró^{32,56}, S. Tripathy^{54,70}, T. Tripathy⁴⁹, S. Trogolo^{34,27}, V. Trubnikov³, W.H. Trzaska¹²⁷, T.P. Trzcinski¹⁴⁴, A. Tumkin¹¹⁰, R. Turrisi⁵⁷, T.S. Tveter²⁰, K. Ullaland²¹, A. Uras¹³⁸, M. Urioni^{58,142}, G.L. Usai²², M. Vala³⁸, N. Valle²⁸, S. Vallero⁶⁰, L.V.R. van Doremalen⁶³, M. van Leeuwen⁹², P. Vande Vyvre³⁴, D. Varga¹⁴⁷, Z. Varga¹⁴⁷, M. Varga-Kofarago¹⁴⁷, M. Vasileiou⁸⁶, A. Vasiliev⁹⁰, O. Vázquez Doce^{52,107}, V. Vechernin¹¹⁴, A. Velure²¹, E. Vercellin²⁴, S. Vergara Limón⁴⁵, L. Vermunt⁶³, R. Vértesi¹⁴⁷, M. Verweij⁶³, L. Vickovic³⁵, Z. Vilakazi¹³³, O. Villalobos Baillie¹¹², G. Vino⁵³, A. Vinogradov⁹⁰, T. Virgili²⁹, V. Vislavicius⁹¹, A. Vodopyanov⁷⁶, B. Volkel^{34,106}, M.A. Völkl¹⁰⁶, K. Voloshin⁹⁴, S.A. Voloshin¹⁴⁵, G. Volpe³³, B. von Haller³⁴, I. Vorobyev¹⁰⁷, N. Vozniuk⁶⁴, J. Vrláková³⁸, B. Wagner²¹, C. Wang⁴⁰, D. Wang⁴⁰, M. Weber¹¹⁵, R.J.G.V. Weelden⁹², A. Wegrzynek³⁴, S.C. Wenzel³⁴, J.P. Wessels¹⁴⁶, J. Wiechula⁶⁹, J. Wikne²⁰, G. Wilk⁸⁷, J. Wilkinson¹⁰⁹, G.A. Willems¹⁴⁶, B. Windelband¹⁰⁶, M. Winn¹⁴⁰, W.E. Witt¹³², J.R. Wright¹²⁰, W. Wu⁴⁰, Y. Wu¹³⁰, R. Xu⁷, A.K. Yadav¹⁴³, S. Yalcin⁷⁸, Y. Yamaguchi⁴⁶, K. Yamakawa⁴⁶, S. Yang²¹, S. Yano⁴⁶, Z. Yin⁷, I.-K. Yoo¹⁷, J.H. Yoon⁶², S. Yuan²¹, A. Yuncu¹⁰⁶, V. Zaccaro²³, C. Zampolli³⁴, H.J.C. Zanoli⁶³, N. Zardoshti³⁴, A. Zarochentsev¹¹⁴, P. Závada⁶⁷, N. Zaviyalov¹¹⁰, M. Zhalov¹⁰⁰, B. Zhang⁷, S. Zhang⁴⁰, X. Zhang⁷, Y. Zhang¹³⁰, V. Zherebchevskii¹¹⁴, Y. Zhi¹¹, N. Zhigareva⁹⁴, D. Zhou⁷, Y. Zhou⁹¹, J. Zhu^{109,7}, Y. Zhu⁷, G. Zinovjev^{3,I}, N. Zurlo^{142,58}

¹ A.I. Alikhanyan National Science Laboratory (Yerevan Physics Institute) Foundation, Yerevan, Armenia

² AGH University of Science and Technology, Cracow, Poland

³ Bogolyubov Institute for Theoretical Physics, National Academy of Sciences of Ukraine, Kiev, Ukraine

⁴ Bose Institute, Department of Physics and Centre for Astroparticle Physics and Space Science (CAPSS), Kolkata, India

⁵ Budker Institute for Nuclear Physics, Novosibirsk, Russia

⁶ California Polytechnic State University, San Luis Obispo, CA, United States

⁷ Central China Normal University, Wuhan, China

⁸ Centro de Aplicaciones Tecnológicas y Desarrollo Nuclear (CEADEN), Havana, Cuba

- ⁹ Centro de Investigación y de Estudios Avanzados (CINVESTAV), Mexico City and Mérida, Mexico
- ¹⁰ Chicago State University, Chicago, IL, United States
- ¹¹ China Institute of Atomic Energy, Beijing, China
- ¹² Chungbuk National University, Cheongju, Republic of Korea
- ¹³ Comenius University Bratislava, Faculty of Mathematics, Physics and Informatics, Bratislava, Slovakia
- ¹⁴ COMSATS University Islamabad, Islamabad, Pakistan
- ¹⁵ Creighton University, Omaha, NE, United States
- ¹⁶ Department of Physics, Aligarh Muslim University, Aligarh, India
- ¹⁷ Department of Physics, Pusan National University, Pusan, Republic of Korea
- ¹⁸ Department of Physics, Sejong University, Seoul, Republic of Korea
- ¹⁹ Department of Physics, University of California, Berkeley, CA, United States
- ²⁰ Department of Physics, University of Oslo, Oslo, Norway
- ²¹ Department of Physics and Technology, University of Bergen, Bergen, Norway
- ²² Dipartimento di Fisica dell'Università and Sezione INFN, Cagliari, Italy
- ²³ Dipartimento di Fisica dell'Università and Sezione INFN, Trieste, Italy
- ²⁴ Dipartimento di Fisica dell'Università and Sezione INFN, Turin, Italy
- ²⁵ Dipartimento di Fisica e Astronomia dell'Università and Sezione INFN, Bologna, Italy
- ²⁶ Dipartimento di Fisica e Astronomia dell'Università and Sezione INFN, Catania, Italy
- ²⁷ Dipartimento di Fisica e Astronomia dell'Università and Sezione INFN, Padova, Italy
- ²⁸ Dipartimento di Fisica e Nucleare e Teorica, Università di Pavia, Pavia, Italy
- ²⁹ Dipartimento di Fisica 'E.R. Caianiello' dell'Università and Gruppo Collegato INFN, Salerno, Italy
- ³⁰ Dipartimento DISAT del Politecnico and Sezione INFN, Turin, Italy
- ³¹ Dipartimento di Scienze e Innovazione Tecnologica dell'Università del Piemonte Orientale and INFN Sezione di Torino, Alessandria, Italy
- ³² Dipartimento di Scienze MIFT, Università di Messina, Messina, Italy
- ³³ Dipartimento Interateneo di Fisica 'M. Merlin' and Sezione INFN, Bari, Italy
- ³⁴ European Organization for Nuclear Research (CERN), Geneva, Switzerland
- ³⁵ Faculty of Electrical Engineering, Mechanical Engineering and Naval Architecture, University of Split, Split, Croatia
- ³⁶ Faculty of Engineering and Science, Western Norway University of Applied Sciences, Bergen, Norway
- ³⁷ Faculty of Nuclear Sciences and Physical Engineering, Czech Technical University in Prague, Prague, Czech Republic
- ³⁸ Faculty of Science, P.J. Šafárik University, Košice, Slovakia
- ³⁹ Frankfurt Institute for Advanced Studies, Johann Wolfgang Goethe-Universität Frankfurt, Frankfurt, Germany
- ⁴⁰ Fudan University, Shanghai, China
- ⁴¹ Gangneung-Wonju National University, Gangneung, Republic of Korea
- ⁴² Gauhati University, Department of Physics, Guwahati, India
- ⁴³ Helmholtz-Institut für Strahlen- und Kernphysik, Rheinische Friedrich-Wilhelms-Universität Bonn, Bonn, Germany
- ⁴⁴ Helsinki Institute of Physics (HIP), Helsinki, Finland
- ⁴⁵ High Energy Physics Group, Universidad Autónoma de Puebla, Puebla, Mexico
- ⁴⁶ Hiroshima University, Hiroshima, Japan
- ⁴⁷ Hochschule Worms, Zentrum für Technologietransfer und Telekommunikation (ZTT), Worms, Germany
- ⁴⁸ Horia Hulubei National Institute of Physics and Nuclear Engineering, Bucharest, Romania
- ⁴⁹ Indian Institute of Technology Bombay (IIT), Mumbai, India
- ⁵⁰ Indian Institute of Technology Indore, Indore, India
- ⁵¹ Indonesian Institute of Sciences, Jakarta, Indonesia
- ⁵² INFN, Laboratori Nazionali di Frascati, Frascati, Italy
- ⁵³ INFN, Sezione di Bari, Bari, Italy
- ⁵⁴ INFN, Sezione di Bologna, Bologna, Italy
- ⁵⁵ INFN, Sezione di Cagliari, Cagliari, Italy
- ⁵⁶ INFN, Sezione di Catania, Catania, Italy
- ⁵⁷ INFN, Sezione di Padova, Padova, Italy
- ⁵⁸ INFN, Sezione di Pavia, Pavia, Italy
- ⁵⁹ INFN, Sezione di Roma, Rome, Italy
- ⁶⁰ INFN, Sezione di Torino, Turin, Italy
- ⁶¹ INFN, Sezione di Trieste, Trieste, Italy
- ⁶² Inha University, Incheon, Republic of Korea
- ⁶³ Institute for Gravitational and Subatomic Physics (GRASP), Utrecht University/Nikhef, Utrecht, Netherlands
- ⁶⁴ Institute for Nuclear Research, Academy of Sciences, Moscow, Russia
- ⁶⁵ Institute of Experimental Physics, Slovak Academy of Sciences, Košice, Slovakia
- ⁶⁶ Institute of Physics, Homi Bhabha National Institute, Bhubaneswar, India
- ⁶⁷ Institute of Physics of the Czech Academy of Sciences, Prague, Czech Republic
- ⁶⁸ Institute of Space Science (ISS), Bucharest, Romania
- ⁶⁹ Institut für Kernphysik, Johann Wolfgang Goethe-Universität Frankfurt, Frankfurt, Germany
- ⁷⁰ Instituto de Ciencias Nucleares, Universidad Nacional Autónoma de México, Mexico City, Mexico
- ⁷¹ Instituto de Física, Universidade Federal do Rio Grande do Sul (UFRGS), Porto Alegre, Brazil
- ⁷² Instituto de Física, Universidad Nacional Autónoma de México, Mexico City, Mexico
- ⁷³ iThemba LABS, National Research Foundation, Somerset West, South Africa
- ⁷⁴ Jeonbuk National University, Jeonju, Republic of Korea
- ⁷⁵ Johann-Wolfgang-Goethe Universität Frankfurt Institut für Informatik, Fachbereich Informatik und Mathematik, Frankfurt, Germany
- ⁷⁶ Joint Institute for Nuclear Research (JINR), Dubna, Russia
- ⁷⁷ Korea Institute of Science and Technology Information, Daejeon, Republic of Korea
- ⁷⁸ KTO Karatay University, Konya, Turkey
- ⁷⁹ Laboratoire de Physique des 2 Infinis, Irène Joliot-Curie, Orsay, France
- ⁸⁰ Laboratoire de Physique Subatomique et de Cosmologie, Université Grenoble-Alpes, CNRS-IN2P3, Grenoble, France
- ⁸¹ Lawrence Berkeley National Laboratory, Berkeley, CA, United States
- ⁸² Lund University Department of Physics, Division of Particle Physics, Lund, Sweden
- ⁸³ Moscow Institute for Physics and Technology, Moscow, Russia
- ⁸⁴ Nagasaki Institute of Applied Science, Nagasaki, Japan
- ⁸⁵ Nara Women's University (NWU), Nara, Japan
- ⁸⁶ National and Kapodistrian University of Athens, School of Science, Department of Physics, Athens, Greece
- ⁸⁷ National Centre for Nuclear Research, Warsaw, Poland
- ⁸⁸ National Institute of Science Education and Research, Homi Bhabha National Institute, Jatni, India

- 89 National Nuclear Research Center, Baku, Azerbaijan
 90 National Research Centre Kurchatov Institute, Moscow, Russia
 91 Niels Bohr Institute, University of Copenhagen, Copenhagen, Denmark
 92 Nikhef, National Institute for Subatomic Physics, Amsterdam, Netherlands
 93 NRC Kurchatov Institute IHEP, Protvino, Russia
 94 NRC «Kurchatov» Institute – ITEP, Moscow, Russia
 95 NRNU Moscow Engineering Physics Institute, Moscow, Russia
 96 Nuclear Physics Group, STFC Daresbury Laboratory, Daresbury, United Kingdom
 97 Nuclear Physics Institute of the Czech Academy of Sciences, Řež u Prahy, Czech Republic
 98 Oak Ridge National Laboratory, Oak Ridge, TN, United States
 99 Ohio State University, Columbus, OH, United States
 100 Petersburg Nuclear Physics Institute, Gatchina, Russia
 101 Physics Department, Faculty of Science, University of Zagreb, Zagreb, Croatia
 102 Physics Department, Panjab University, Chandigarh, India
 103 Physics Department, University of Jammu, Jammu, India
 104 Physics Department, University of Rajasthan, Jaipur, India
 105 Physikalisches Institut, Eberhard-Karls-Universität Tübingen, Tübingen, Germany
 106 Physikalisches Institut, Ruprecht-Karls-Universität Heidelberg, Heidelberg, Germany
 107 Physik Department, Technische Universität München, Munich, Germany
 108 Politecnico di Bari and Sezione INFN, Bari, Italy
 109 Research Division and ExtreMe Matter Institute EMMI, GSI Helmholtzzentrum für Schwerionenforschung GmbH, Darmstadt, Germany
 110 Russian Federal Nuclear Center (VNIIEF), Sarov, Russia
 111 Saha Institute of Nuclear Physics, Homi Bhabha National Institute, Kolkata, India
 112 School of Physics and Astronomy, University of Birmingham, Birmingham, United Kingdom
 113 Sección Física, Departamento de Ciencias, Pontificia Universidad Católica del Perú, Lima, Peru
 114 St. Petersburg State University, St. Petersburg, Russia
 115 Stefan Meyer Institut für Subatomare Physik (SMI), Vienna, Austria
 116 SUBATECH, IMT Atlantique, Université de Nantes, CNRS-IN2P3, Nantes, France
 117 Suranaree University of Technology, Nakhon Ratchasima, Thailand
 118 Technical University of Košice, Košice, Slovakia
 119 The Henryk Niewodniczanski Institute of Nuclear Physics, Polish Academy of Sciences, Cracow, Poland
 120 The University of Texas at Austin, Austin, TX, United States
 121 Universidad Autónoma de Sinaloa, Culiacán, Mexico
 122 Universidade de São Paulo (USP), São Paulo, Brazil
 123 Universidade Estadual de Campinas (UNICAMP), Campinas, Brazil
 124 Universidade Federal do ABC, Santo Andre, Brazil
 125 University of Cape Town, Cape Town, South Africa
 126 University of Houston, Houston, TX, United States
 127 University of Jyväskylä, Jyväskylä, Finland
 128 University of Kansas, Lawrence, KS, United States
 129 University of Liverpool, Liverpool, United Kingdom
 130 University of Science and Technology of China, Hefei, China
 131 University of South-Eastern Norway, Tonsberg, Norway
 132 University of Tennessee, Knoxville, TN, United States
 133 University of the Witwatersrand, Johannesburg, South Africa
 134 University of Tokyo, Tokyo, Japan
 135 University of Tsukuba, Tsukuba, Japan
 136 University Politehnica of Bucharest, Bucharest, Romania
 137 Université Clermont Auvergne, CNRS/IN2P3, LPC, Clermont-Ferrand, France
 138 Université de Lyon, CNRS/IN2P3, Institut de Physique des 2 Infinis de Lyon, Lyon, France
 139 Université de Strasbourg, CNRS, IPHC UMR 7178, F-67000 Strasbourg, France
 140 Université Paris-Saclay Centre d'Etudes de Saclay (CEA), IRFU, Département de Physique Nucléaire (DPhN), Saclay, France
 141 Università degli Studi di Foggia, Foggia, Italy
 142 Università di Brescia, Brescia, Italy
 143 Variable Energy Cyclotron Centre, Homi Bhabha National Institute, Kolkata, India
 144 Warsaw University of Technology, Warsaw, Poland
 145 Wayne State University, Detroit, MI, United States
 146 Westfälische Wilhelms-Universität Münster, Institut für Kernphysik, Münster, Germany
 147 Wigner Research Centre for Physics, Budapest, Hungary
 148 Yale University, New Haven, CT, United States
 149 Yonsei University, Seoul, Republic of Korea

^I Deceased.

^{II} Also at: Italian National Agency for New Technologies, Energy and Sustainable Economic Development (ENEA), Bologna, Italy.

^{III} Also at: Dipartimento DET del Politecnico di Torino, Turin, Italy.

^{IV} Also at: M.V. Lomonosov Moscow State University, D.V. Skobel'syn Institute of Nuclear, Physics, Moscow, Russia.

^V Also at: Department of Applied Physics, Aligarh Muslim University, Aligarh, India.

^{VI} Also at: Institute of Theoretical Physics, University of Wrocław, Poland.

^{VII} Also at: University of Kansas, Lawrence, Kansas, United States.